BIT manuscript No.
(will be inserted by the editor)

A stochastic exponential Euler scheme for simulation of stiff biochemical reaction systems

Yoshio Komori · **Kevin Burrage**

Received: date / Accepted: date

Abstract In order to simulate stiff biochemical reaction systems, an explicit exponential Euler scheme is derived for multi-dimensional, non-commutative stochastic differential equations with a semilinear drift term. The scheme is of strong order one half and A-stable in mean square. The combination with this and the projection method shows good performance in numerical experiments dealing with an alternative formulation of the chemical Langevin equation for a human ether a-go-go related gene ion channel model.

Keywords Explicit method · Mean square stability · Chemical Langevin equation

Mathematics Subject Classification (2000) 60H10 · 60H35 · 65C30 · 92-08

1 Introduction

While it has been customary to treat the numerical solution of stiff ordinary differential equations (ODEs) by implicit methods, there are some classes of explicit methods that are well suited to solving some types of stiff problems. One such class is the

An initial presentation relating to this work was given in the 19th IMACS World Congress. This work was partially supported by JSPS Grant-in-Aid for Scientific Research No. 23540143. It was also partially supported by Kyushu Institute of Technology through subsidies for educational employees on the overseas study program.

Yoshio Komori
Department of Systems Design and Informatics, Kyushu Institute of Technology, Iizuka, 820-8502, Japan
Tel.: +81-948-7731
Fax: +81-948-7709
E-mail: komori@ces.kyutech.ac.jp, yoshio.kom@gmail.com

Kevin Burrage
Department of Computer Science, University of Oxford, Wolfson Building, Parks Road, Oxford, OX1 3QD, UK
Discipline of Mathematics, Queensland University of Technology, Brisbane, QLD 4001, Australia
E-mail: kevin.burrage@cs.ox.ac.uk, kevin.burrage@gmail.com

class of Runge-Kutta Chebyshev (RKC) methods. They are useful for stiff problems whose eigenvalues lie near the negative real axis. An original contribution is given by van der Houwen and Sommeijer [22] who have constructed explicit s-stage Runge-Kutta (RK) methods whose stability functions are shifted Chebyshev polynomials $T_s(1+z/s^2)$. These have stability regions along the negative real axis of $[-2s^2,0]$. In order to achieve second or fourth order, this class of methods has been modified by Abdulle and Medovikov [4] and Abdulle [1], respectively. Note that these methods need to increase the stage number s for stabilization. Another suitable class of methods is the class of explicit exponential RK methods for semilinear problems [16, 19–21, 32, 36]. Although these methods were proposed many years ago, until recently they have not been regarded as practical because of the cost of calculations for matrix exponentials, especially for large problems. In order to overcome this problem, new methods have been proposed [19–21]. Note that explicit exponential RK methods are A-stable.

Similarly, for stochastic differential equations (SDEs) stabilized explicit RK methods have been developed. An original contribution concerning RKC methods is by Abdulle and his colleagues [2, 3] who have developed a family of explicit stochastic orthogonal Runge-Kutta Chebyshev (SROCK) methods with extended mean square (MS) stability regions. Their methods have strong order one half and weak order one for non-commutative Stratonovich and Itô SDEs, whereas they reduce to the first order RKC methods when applied to ODEs. By developing their ideas, Komori and Burrage [30, 31] have proposed weak second order SROCK methods for non-commutative Stratonovich SDEs and strong first order SROCK methods for non-commutative Itô and Stratonovich SDEs. They reduce to the first or second order RKC methods when applied to ODEs. Note that these methods also need to increase the stage number for stabilization. In addition, a class of exponential integrators for SDEs, known as Local Linearization (LL) methods, has been proposed by Jimenez [25–27] and Cruz [14] for the strong approximation to solutions of SDEs with additive noise, whereas Biscay [9] and Shoji [39] have considered LL methods for scalar SDEs with multiplicative noise driven by a scalar Wiener process. Mora [34] and Carbonell, Jimenez and Biscay [12] have also proposed LL methods for the weak approximation to solutions of SDEs with additive noise. Shi, Xiao and Zhang [38] have considered an exponential Euler scheme for the strong approximation to solutions of SDEs with multiplicative noise driven by a scalar Wiener process. In addition, exponential integrators have been considered for stochastic partial differential equations with a semilinear drift term and additive noise [24] or multiplicative noise [5].

In biochemical kinetics, the chemical Langevin equation (CLE) is an important modelling framework and it plays an intermediate role between the chemical master equation and the reaction rate equation for biochemical simulation [17, 23, 33]. The CLE consists of a system of Itô SDEs with non-commutative noise. In a seminal paper Gillespie [17] has derived an original form of the CLE. Mélykúti, Burrage and Zygalakis [33] have considered other possible forms and have derived a computationally effective form that needs fewer Wiener increments than that in Gillespie's original formulation. In order for simulation of the CLE to be biological meaningful, approximate solutions have to be non-negative and they are often required to satisfy other boundary conditions. Dangerfield, Kay and Burrage [15] have proposed tack-

ling such problems by the use of reflected SDEs [40,41] and the projection method [13]. Although the issue of non-negativity and weak approximations are often dealt with for a specific type of SDEs also in the field of finance [6], note that strong approximations are essential in our problems.

In the present paper we shall put all these ideas together. In using projection method, numerical methods with one intermediate stage are the most favourable and so we will derive an explicit exponential Euler scheme for multi-dimensional, non-commutative Itô SDEs with a semilinear drift term. The scheme together with the projection method will show very good performance for stiff biochemical problems. In Section 2 we will introduce the exponential Euler scheme for ODEs and derive the exponential Euler scheme for SDEs. After that, we will investigate its MS stability. Section 3 will present numerical results and Section 4 our conclusions.

2 Exponential schemes

2.1 Exponential Euler scheme

We consider autonomous semilinear ODEs given by

$$\boldsymbol{y}'(t) = A\boldsymbol{y}(t) + \boldsymbol{f}(\boldsymbol{y}(t)), \qquad t > 0, \qquad \boldsymbol{y}(0) = \boldsymbol{y}_0, \tag{2.1}$$

where $\boldsymbol{y}$ is an $\mathbb{R}^d$-valued function on $[0,\infty)$, A is a $d \times d$ matrix and $\boldsymbol{f}$ is an $\mathbb{R}^d$-valued nonlinear function on $\mathbb{R}^d$ or a constant vector. By the variation-of-constants formula, the exact solution of (2.1) is represented as

$$\boldsymbol{y}(t) = \mathrm{e}^{At}\boldsymbol{y}_0 + \int_0^t \mathrm{e}^{A(t-s)}\boldsymbol{f}(\boldsymbol{y}(s))\mathrm{d}s. \tag{2.2}$$

When $\boldsymbol{y}_n$ denotes a discrete approximation to the solution $\boldsymbol{y}(t_n)$ of (2.1) for an equidistant grid point $t_n \overset{\text{def}}{=} nh$ ($n = 1,2,\ldots,M$) with step size h (M is a natural number), we can derive a numerical scheme by utilizing (2.2). From (2.2), we have

$$\boldsymbol{y}(t_{n+1}) = \mathrm{e}^{Ah}\boldsymbol{y}_n + \int_{t_n}^{t_{n+1}} \mathrm{e}^{A(t_{n+1}-s)}\boldsymbol{f}(\boldsymbol{y}(s))\mathrm{d}s$$

if $\boldsymbol{y}(t_n) = \boldsymbol{y}_n$. By interpolating $\boldsymbol{f}(\boldsymbol{y}(s))$ at $\boldsymbol{f}(\boldsymbol{y}_n)$ only, we obtain the simplest exponential scheme for (2.1) [21]:

$$\boldsymbol{y}_{n+1} = \mathrm{e}^{Ah}\boldsymbol{y}_n + \varphi_1(Ah)\boldsymbol{f}(\boldsymbol{y}_n)h, \tag{2.3}$$

where $\varphi_1(Z) \overset{\text{def}}{=} Z^{-1}(e^Z - I)$ and I stands for the $d \times d$ identity matrix. This is called the exponential Euler scheme.

When we apply (2.3) to the scalar test equation

$$y'(t) = \lambda y(t), \quad t > 0, \quad y(0) = y_0, \tag{2.4}$$

where $\Re(\lambda) \leq 0$ and $y_0 \neq 0$, we have $y_{n+1} = R(\lambda h)y_n$ for which $R(z) = \mathrm{e}^z$. Thus, although (2.3) is an explicit scheme, it is A-stable, that is, its stability region $\{z \mid |R(z)| \leq 1\}$ contains the whole left half of the complex plane [11].

2.2 Exponential Euler scheme for SDEs

Similarly to the previous subsection, we are concerned with autonomous SDEs with the semilinear drift term given by

$$\mathrm{d}\boldsymbol{y}(t) = (A\boldsymbol{y}(t) + \boldsymbol{f}(\boldsymbol{y}(t)))\mathrm{d}t + \sum_{j=1}^{m} \boldsymbol{g}_j(\boldsymbol{y}(t))\mathrm{d}W_j(t), \qquad t > 0, \qquad \boldsymbol{y}(0) = \boldsymbol{y}_0, \quad (2.5)$$

where $\boldsymbol{g}_j$, $j = 1, 2, \ldots, m$ are $\mathbb{R}^d$-valued functions on $\mathbb{R}^d$, the $W_j(t)$, $j = 1, 2, \ldots, m$ are independent Wiener processes and $\boldsymbol{y}_0$ is independent of $W_j(t) - W_j(0)$ for $t > 0$. If a global Lipschitz condition is satisfied, the stochastic differential equation (SDE) has exactly one continuous global solution on the entire interval $[0, \infty)$ [7, p. 113].

Similarly to (2.1), the exact solution of (2.5) is represented by

$$\boldsymbol{y}(t) = \mathrm{e}^{At}\boldsymbol{y}_0 + \int_0^t \mathrm{e}^{A(t-s)}\boldsymbol{f}(\boldsymbol{y}(s))\mathrm{d}s + \sum_{j=1}^{m} \int_0^t \mathrm{e}^{A(t-s)}\boldsymbol{g}_j(\boldsymbol{y}(s))\mathrm{d}W_j(s)$$

(see also [5, 38]). We can derive numerical schemes by utilizing this. From it, we have

$$\begin{aligned}\boldsymbol{y}(t_{n+1}) = \mathrm{e}^{Ah}\boldsymbol{y}_n &+ \int_{t_n}^{t_{n+1}} \mathrm{e}^{A(t_{n+1}-s)}\boldsymbol{f}(\boldsymbol{y}(s))\mathrm{d}s \\ &+ \sum_{j=1}^{m} \int_{t_n}^{t_{n+1}} \mathrm{e}^{A(t_{n+1}-s)}\boldsymbol{g}_j(\boldsymbol{y}(s))\mathrm{d}W_j(s) \end{aligned} \quad (2.6)$$

if $\boldsymbol{y}(t_n) = \boldsymbol{y}_n$. If we simply choose the left-hand point of the interval to approximate the integrals in both of the drift and diffusion terms, we have

$$\boldsymbol{y}_{n+1} = \mathrm{e}^{Ah}\boldsymbol{y}_n + \mathrm{e}^{Ah}\boldsymbol{f}(\boldsymbol{y}_n)h + \mathrm{e}^{Ah}\sum_{j=1}^{m} \boldsymbol{g}_j(\boldsymbol{y}_n)\triangle W_j \quad (2.7)$$

as an approximation to $\boldsymbol{y}(t_{n+1})$, where $\triangle W_j \stackrel{\mathrm{def}}{=} W_j(t_{n+1}) - W_j(t_n)$. For $m = 1$ (2.7) is the same as an exponential Euler scheme proposed by Shi et al. [38] for SDEs with a scalar Wiener process. When (2.7) is applied to ODEs, it is equivalent to the Lawson-Euler scheme [32, 38]. In addition, it has a similar type of approximations in both of the drift and diffusion terms. Thus, let us call it the stochastic Lawson-Euler (SLE) scheme in the sequel.

For (2.6), if we interpolate $\boldsymbol{f}(\boldsymbol{y}(s))$ at $\boldsymbol{f}(\boldsymbol{y}_n)$ similarly to (2.3) and choose the left-hand point of the interval in the diffusion terms similarly to (2.7), then we have

$$\boldsymbol{y}_{n+1} = \mathrm{e}^{Ah}\boldsymbol{y}_n + \varphi_1(Ah)\boldsymbol{f}(\boldsymbol{y}_n)h + \mathrm{e}^{Ah}\sum_{j=1}^{m} \boldsymbol{g}_j(\boldsymbol{y}_n)\triangle W_j. \quad (2.8)$$

Adamu [5] has proposed this scheme and has called it the SETD0 scheme. (SETD stands for "stochastic exponential time differencing".)

When we interpolate $\boldsymbol{f}(\boldsymbol{y}(s))$ at $\boldsymbol{f}(\boldsymbol{y}_n)$ similarly to (2.3) and also interpolate $\boldsymbol{g}_j(\boldsymbol{y}(s))$ at $\boldsymbol{g}_j(\boldsymbol{y}_n)$ in (2.6), we obtain the following approximation to $\boldsymbol{y}(t_{n+1})$:

$$\boldsymbol{y}(t_{n+1}) \simeq \mathrm{e}^{Ah}\boldsymbol{y}_n + \varphi_1(Ah)\boldsymbol{f}(\boldsymbol{y}_n)h + \sum_{j=1}^{m} \left(\int_{t_n}^{t_{n+1}} \mathrm{e}^{A(t_{n+1}-s)}\mathrm{d}W_j(s) \right) \boldsymbol{g}_j(\boldsymbol{y}_n).$$

In [39], another approximation was considered for scalar SDEs. In order to approximate the stochastic integrals in the right-hand side, let us consider an approximation

$$\int_{t_n}^{t_{n+1}} \alpha \mathrm{d}W_j(s) \tag{2.9}$$

to $\int_{t_n}^{t_{n+1}} \mathrm{e}^{a(t_{n+1}-s)}\mathrm{d}W_j(s)$, where $a \in \mathbb{R}$. Because its MS error is given by

$$E\left[\left\{\int_{t_n}^{t_{n+1}} \left(\mathrm{e}^{a(t_{n+1}-s)}-\alpha\right)\mathrm{d}W_j(s)\right\}^2\right] = \int_{t_n}^{t_{n+1}} \left(\mathrm{e}^{a(t_{n+1}-s)}-\alpha\right)^2 \mathrm{d}s,$$

by differentiating this with respect to α and setting it at zero, we obtain

$$\alpha = (ah)^{-1}\left(\mathrm{e}^{ah}-1\right). \tag{2.10}$$

Hence, we can derive the following scheme:

$$\boldsymbol{y}_{n+1} = \mathrm{e}^{Ah}\boldsymbol{y}_n + \varphi_1(Ah)\boldsymbol{f}(\boldsymbol{y}_n)h + \varphi_1(Ah)\sum_{j=1}^{m}\boldsymbol{g}_j(\boldsymbol{y}_n)\triangle W_j. \tag{2.11}$$

When (2.11) is applied to ODEs, it is equivalent to the exponential Euler scheme. In addition, it has a similar type of approximations in both of the drift and diffusion terms. Thus, let us call it the stochastic exponential Euler (SEE) scheme.

In general, when discrete approximations $\boldsymbol{y}_n$ are given by a numerical scheme, we say that the scheme is of strong order p if there exists a constant C such that

$$\left(E[||\boldsymbol{y}_M - \boldsymbol{y}(T)||^2]\right)^{1/2} \leq Ch^p \tag{2.12}$$

with $T = Mh$ and h sufficiently small [29,37], where $||\cdot||$ stands for the Euclidean norm. Here, remember that we have already given some notations in Subsection 2.1. Let us assume $\boldsymbol{f}, \boldsymbol{g}_j \in \boldsymbol{C}^2$ for $j = 1,2,\ldots,m$. Then, it is known that the Euler-Maruyama (EM) scheme for solving (2.5)

$$\boldsymbol{y}_{n+1} = \boldsymbol{y}_n + (A\boldsymbol{y}_n + \boldsymbol{f}(\boldsymbol{y}_n))h + \sum_{j=1}^{m}\boldsymbol{g}_j(\boldsymbol{y}_n)\triangle W_j \tag{2.13}$$

is of strong order one half [29,37].

The following points can be made.

- When A goes to the zero matrix, (2.11) is equivalent to the EM scheme.
- Because the expression on the right-hand side of (2.11) can be truncated in the following form

$$\begin{aligned}\boldsymbol{y}_{n+1} = \boldsymbol{y}_n &+ (A\boldsymbol{y}_n + \boldsymbol{f}(\boldsymbol{y}_n))h + \sum_{j=1}^{m}\boldsymbol{g}_j(\boldsymbol{y}_n)\triangle W_j \\ &+ \frac{1}{2}A(A\boldsymbol{y}_n + \boldsymbol{f}(\boldsymbol{y}_n))h^2 + \frac{1}{2}Ah\sum_{j=1}^{m}\boldsymbol{g}_j(\boldsymbol{y}_n)\triangle W_j\end{aligned}$$

  for a small h, (2.11) is also of strong order one half.

- It is reasonable to approximate $e^{a(t_{n+1}-s)}$ by the constant α in (2.9) as even $\int_{t_n}^{t_{n+1}} s dW_j(s)$ is of order one and one half in MS.
- For (2.10), (2.9) obeys the normal distribution with mean 0 and variance

$$\int_{t_n}^{t_{n+1}} \alpha^2 ds = \frac{1}{a^2 h}\left(e^{ah}-1\right)^2 = h + ah^2 + \frac{7}{12}a^2h^3 + O(h^4),$$

whereas $\int_{t_n}^{t_{n+1}} e^{a(t_{n+1}-s)} dW_j(s)$ obeys the normal distribution with mean 0 and variance

$$\int_{t_n}^{t_{n+1}} e^{2a(t_{n+1}-s)} ds = \frac{1}{2a}\left(e^{2ah}-1\right) = h + ah^2 + \frac{2}{3}a^2h^3 + O(h^4).$$

In [5, 39], another approximation was considered for the stochastic integral and it finally led to the square root of a matrix exponential function.

2.3 MS stability analysis for the SEE scheme

As with the deterministic case, if we apply (2.11) to the scalar test equation [18]

$$dy(t) = \lambda y(t)dt + \sum_{j=1}^{m} \sigma_j y(t) dW_j(t), \qquad t > 0, \qquad y(0) = y_0, \tag{2.14}$$

where $y_0 \neq 0$ with probability one (w. p. 1) and where λ and σ_j $(1 \leq j \leq m)$ are complex values and they satisfy

$$2\Re(\lambda) + \sum_{j=1}^{m} |\sigma_j|^2 < 0, \tag{2.15}$$

then, we have

$$y_{n+1} = R\left(\lambda h, \sum_{j=1}^{m} \sigma_j \triangle W_j\right) y_n$$

for which $R(z,w) = e^z + z^{-1}(e^z - 1)w$.

Because of (2.15), the solution of (2.14) is MS stable ($\lim_{t\to\infty} E[|y(t)|^2] = 0$) [18]. On the other hand, the MS stability function $\hat{R}$ of (2.11) is given by

$$\begin{aligned}\hat{R}(p_r, p_i, q) &\stackrel{\text{def}}{=} E\left[\left|R\left(\lambda h, \sum_{j=1}^{m} \sigma_j \triangle W_j\right)\right|^2\right] \\ &= e^{2p_r} + \frac{\left(e^{2p_r} - 2e^{p_r}\cos p_i + 1\right) q}{p_r^2 + p_i^2}\end{aligned} \tag{2.16}$$

where $p_r \stackrel{\text{def}}{=} \Re(\lambda)h$, $p_i \stackrel{\text{def}}{=} \Im(\lambda)h$ and $q \stackrel{\text{def}}{=} \sum_{j=1}^{m} |\sigma_j|^2 h$. The MS stability ($E[|y_n|^2] \to 0$ $(n \to \infty)$) for (2.11) is equivalent to $\hat{R}(p_r, p_i, q) < 1$ [18]. Thus, the MS stability domain of (2.11) is defined by $\{(p_r, p_i, q) \mid \hat{R}(p_r, p_i, q) < 1\}$.

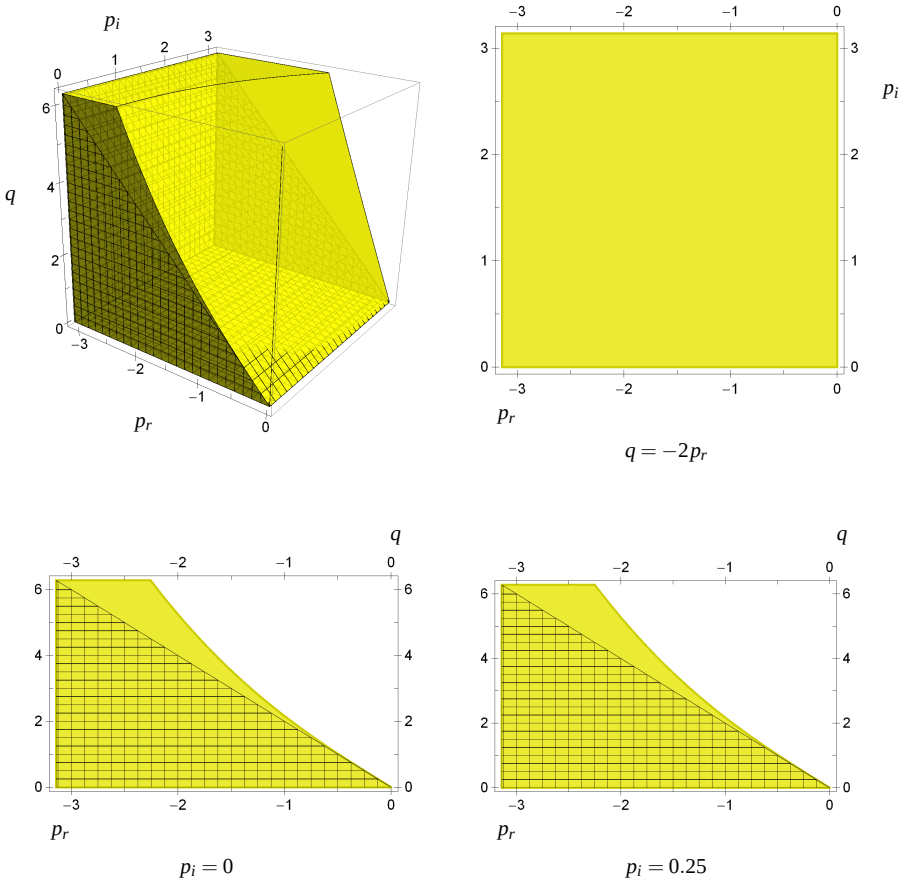

Fig. 2.1 MS stability domain (top left) and its profiles (top right and bottom) for the SEE scheme

We can rewrite (2.15) as $2p_r + q < 0$. Using this, we obtain

$$\hat{R}(p_r, p_i, q) < \tilde{R}(p_r, p_i) \stackrel{\text{def}}{=} \mathrm{e}^{2p_r} - \frac{2p_r\left(\mathrm{e}^{2p_r} - 2\mathrm{e}^{p_r}\cos p_i + 1\right)}{p_r^2 + p_i^2}, \tag{2.17}$$

from (2.16).

First, let us consider the case of $p_i = 0$. As

$$\tilde{R}(p_r, 0) = \frac{(p_r - 2)\mathrm{e}^{2p_r} + 4\mathrm{e}^{p_r} - 2}{p_r},$$

we have $\lim_{p_r \to -0} \tilde{R}(p_r, 0) = 1$ and $\tilde{R}(p_r, 0)$ is a monotone increasing function of p_r. Thus, $\tilde{R}(p_r, 0) < 1$ for $p_r < 0$.

Next, let us consider the case of $p_i \geq \pi$. In this case, we have

$$\tilde{R}(p_r, p_i) \leq \frac{(p_r^2 - 2p_r + \pi^2)\mathrm{e}^{2p_r} - 4p_r\mathrm{e}^{p_r} - 2p_r}{p_r^2 + \pi^2}.$$

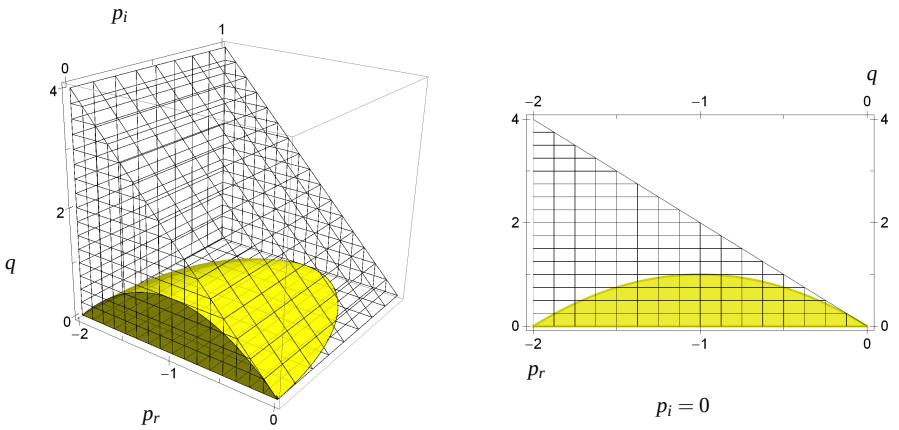

Fig. 2.2 MS stability domain (left) and its profile (right) for the EM scheme

When we denote by $\psi_1(p_r)$ the expression in the right-hand side, we have $\psi_1(0) = 1$ and

$$\psi_1'(p_r) = 2\frac{\left\{\left(p_r^2+\pi^2+\pi\right)\mathrm{e}^{p_r} - p_r + \pi\right\}u(p_r) - 2p_r\left(p_r^2+\pi^2\right)\mathrm{e}^{2p_r} + p_r^2\left(\mathrm{e}^{p_r}+2\right)\mathrm{e}^{p_r}}{\left(p_r^2+\pi^2\right)^2},$$

where

$$u(p_r) \stackrel{\text{def}}{=} \left(p_r^2+\pi^2-\pi\right)\mathrm{e}^{p_r} - p_r - \pi.$$

As $u'(0) > 0$, $\lim_{p_r\to-\infty} u'(p_r) = -1$ and $u''(p_r) > 0$, $u(p_r)$ is a convex function and it reaches its minimum value at a point, say, β, in the interval $(-\infty, 0]$. We can numerically obtain $\beta = -1.869$ and $u(\beta) = 0.304$. Thus, $u(p_r) > 0$ holds for $p_r \le 0$. This fact leads to $\tilde{R}(p_r, p_i) < 1$ for $p_r \le 0$ and $p_i \ge \pi$.

As $\hat{R}(p_r, p_i, q) = \hat{R}(p_r, -p_i, q)$, all that remains is the case of $\pi > p_i > 0$. Let $\psi_2(p_r)$ be $\tilde{R}(p_r, \varepsilon)$ for a positive $\varepsilon < \pi$. Then, since $\psi_2'(p_r) > 0$ for $p_r \le -\varepsilon$, we have $\psi_2(p_r) \le \psi_2(-\pi)$ for $p_r \le -\pi$, which implies $\tilde{R}(p_r, \varepsilon) \le \tilde{R}(-\pi, \varepsilon)$. On the other hand, $\tilde{R}(-\pi, p_i)$ is a monotone decreasing function of p_i when $0 < p_i < \pi$, and $\tilde{R}(-\pi, 0) < 1$. Thus, $\tilde{R}(p_r, p_i) < 1$ for $p_r \le -\pi$ and $0 < p_i < \pi$. Consequently, we plot the MS stability domain for $-\pi < p_r < 0$ and $0 < p_i < \pi$.

The MS stability domain and its profiles are given in Figure 2.1. The MS stability domain is indicated by the colored part in the top left of the figure. Here, the other part enclosed by the mesh indicates the domain in which the solution of the test SDE is MS stable. In the bottom of the figure, the colored area indicates the profile of the MS stability domain when $p_i = 0$ or 0.25, whereas the area enclosed by the mesh indicates the region in which the solution of the test SDE is MS stable. In the top right of the figure, the colored area indicates the profile of the MS stability domain when $q = -2p_r$, which is the boundary of the stability region of the test SDE. From these results, we can see that the SEE scheme is A-stable in MS [18], that is, its stability domain contains the domain that satisfies $2p_r + q < 0$.

For comparisons, lastly let us check the stability of the EM scheme. When (2.13) is applied to (2.14), the MS stability function of (2.13) is given by

$$\hat{R}(p_r, p_i, q) = (1+p_r)^2 + p_i^2 + q.$$

The MS stability domain and its profile are given in Figures 2.2. Note that the colorless part or area enclosed by the mesh indicates situations in which the solution of the test SDE is MS stable, but the numerical solution by the EM scheme is not.

3 Simulation for a K^+ channel

3.1 Reflected SDEs and projection method

When (2.5) is considered for biological simulation, one of the critical problems often leads to keeping the non-negativity of $y_i(t)$ $(i = 1, 2, \ldots, d)$ and conserving the sum of them because of having biological meaning – the components y_i's represent chemical concentrations. Let us denote by D the hyperplane given by $\sum_{i=1}^{d} y_i(t) = L$ for an $L > 0$ which lies inside the hypercube bounded by the intervals $[0, L]$, and by ∂D the boundary of D. In order to overcome the problem, Dangerfield et al. [15] have proposed using reflected SDEs [40, 41] instead of directly using (2.5). The reflected SDEs are given by the following form:

$$\begin{aligned} &\mathrm{d}\boldsymbol{y}(t) = (A\boldsymbol{y}(t) + \boldsymbol{f}(\boldsymbol{y}(t)))\mathrm{d}t + \sum_{j=1}^{m} \boldsymbol{g}_j(\boldsymbol{y}(t))\mathrm{d}W_j(t) + \mathrm{d}\boldsymbol{r}(t), \qquad t > 0, \\ &\boldsymbol{y}(0) = \boldsymbol{y}_0 \end{aligned} \tag{3.1}$$

with the properties [8, 15]

$$|\boldsymbol{r}|(t) = \int_0^t \boldsymbol{1}_{\{\boldsymbol{y}(s) \in \partial D\}} \mathrm{d}|\boldsymbol{r}|(s), \qquad \boldsymbol{r}(t) = \int_0^t \nu(s)\mathrm{d}|\boldsymbol{r}|(s), \tag{3.2}$$

where $\boldsymbol{1}$ stands for an indicator function, $\nu(s) \in N(\boldsymbol{y}(s))$ if $\boldsymbol{y}(s) \in \partial D$ and $N(\boldsymbol{a})$ is the set of inward pointing unit vectors to the point $\boldsymbol{a}$ that lies on ∂D. As a numerical method to solve reflected SDEs, Dangerfield et al. [15] have adopted the projection method, rather than penalization methods. Although the solution of (3.1) is a pair $(\boldsymbol{y}(t), \boldsymbol{r}(t))$ that satisfies (3.2) [35, 42], the projection method can give numerical solutions without explicitly performing calculations for the reflecting process $\boldsymbol{r}(t)$.

The projection method is described as follows. When we have an approximate solution $\boldsymbol{y}_n \in D$ at time t_n, from this we calculate an unreflected approximate solution, say $\boldsymbol{y}_{n+1}^{(un)}$, by using the EM scheme or an exponential scheme. If $\boldsymbol{y}_{n+1}^{(un)} \in D$, we use this as an approximate solution $\boldsymbol{y}_{n+1}$ at time t_{n+1}. If not, we use the projection of $\boldsymbol{y}_{n+1}^{(un)}$ onto ∂D. When $\Pi(\cdot)$ denotes the projection, this procedure can be rewritten as

$$\boldsymbol{y}_{n+1} = \begin{cases} \boldsymbol{y}_{n+1}^{(un)} & \text{if } \boldsymbol{y}_{n+1}^{(un)} \in D, \\ \Pi(\boldsymbol{y}_{n+1}^{(un)}) & \text{if } \boldsymbol{y}_{n+1}^{(un)} \notin D. \end{cases}$$

Chen and Ye [13] have proposed the algorithm that gives $\Pi(\boldsymbol{y}_{n+1}^{(un)})$ as follows:

1) Set $\boldsymbol{u} := \boldsymbol{y}_{n+1}^{(un)}$, where $\boldsymbol{y}_{n+1}^{(un)}$ is an approximate solution to (2.5) calculated by the EM scheme or an exponential scheme.
2) Sort the elements of $\boldsymbol{u}$ in the ascending order as $u_{(1)} \leq u_{(2)} \leq \cdots \leq u_{(d)}$, and set $i := d-1$.
3) Set s_i by
$$s_i := \frac{1}{d-i}\left(\sum_{k=i+1}^{d} u_{(k)} - L\right).$$
If $s_i \geq u_{(i)}$, then set $\hat{s} := s_i$ and go to Step 5). Otherwise, set $i := i-1$ and redo Step 3) if $i \geq 1$ or go to Step 4) if $i = 0$.
4) Set $\hat{s}$ by
$$\hat{s} := \frac{1}{d}\left(\sum_{k=1}^{d} u_{(k)} - L\right).$$
5) Return
$$[\max(u_1 - \hat{s}, 0)\ \max(u_2 - \hat{s}, 0)\ \cdots\ \max(u_d - \hat{s}, 0)]^\top$$
as the projection of $\boldsymbol{u}$, where $u_1, u_2, \ldots, u_d$ are the unsorted elements of $\boldsymbol{u}$.

For more details including the error analysis of the projection method, see [15].

3.2 State space reduction

As an example of real interest to biologists, we consider a model for a human ether a-go-go related gene K^+ ion channel [10,28]. Mélykúti et al. [33] have given the Langevin formulation of this model. The model has three closed states, one open state and one inactivation state as five chemical species reacting through ten reactions, and takes the form

$$A = \begin{bmatrix} -k_1 & k_2 & 0 & 0 & 0 \\ k_1 & -k_2-k_3 & k_4 & 0 & 0 \\ 0 & k_3 & -k_4-k_5-k_{10} & k_6 & k_9 \\ 0 & 0 & k_5 & -k_6-k_7 & k_8 \\ 0 & 0 & k_{10} & k_7 & -k_8-k_9 \end{bmatrix}, \tag{3.3}$$

$$\boldsymbol{f}(\boldsymbol{y}) = \begin{bmatrix} 0\ 0\ 0\ 0\ 0 \end{bmatrix}^\top,$$

$$\begin{bmatrix} \boldsymbol{g}_1(\boldsymbol{y})\ \boldsymbol{g}_2(\boldsymbol{y})\ \boldsymbol{g}_3(\boldsymbol{y})\ \boldsymbol{g}_4(\boldsymbol{y})\ \boldsymbol{g}_5(\boldsymbol{y}) \end{bmatrix}$$
$$= \begin{bmatrix} -1 & 0 & 0 & 0 & 0 \\ 1 & -1 & 0 & 0 & 0 \\ 0 & 1 & -1 & 0 & 1 \\ 0 & 0 & 1 & -1 & 0 \\ 0 & 0 & 0 & 1 & -1 \end{bmatrix} \operatorname{diag}\begin{pmatrix} \sqrt{k_1 y_1 + k_2 y_2} \\ \sqrt{k_3 y_2 + k_4 y_3} \\ \sqrt{k_5 y_3 + k_6 y_4} \\ \sqrt{k_7 y_4 + k_8 y_5} \\ \sqrt{k_9 y_5 + k_{10} y_3} \end{pmatrix}$$

with the conditions $0 \leq y_i(t) \leq L$ $(i = 1,2,\ldots,5)$ and

$$\sum_{i=1}^{5} y_i(t) = L, \tag{3.4}$$

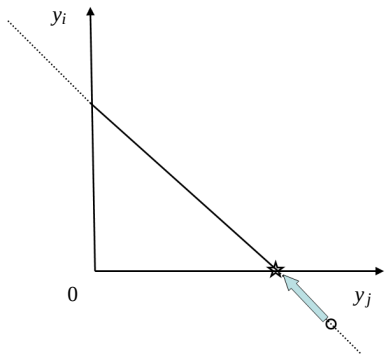

Fig. 3.1 Diagrammatical representation of how the projection method works for our formulation

where $L = \sum_{i=1}^{5} y_i(0)$. Because the rank of A is four in (3.3), we cannot apply (2.8) or (2.11) to this formulation. We have to reduce the number of state variables.

When we set U as

$$U \stackrel{\text{def}}{=} \begin{bmatrix} 1&0&0&0&0 \\ 0&1&0&0&0 \\ 0&0&1&0&0 \\ 0&0&0&1&0 \\ 1&1&1&1&1 \end{bmatrix},$$

left multiplication by U does not change the first four rows of A and

$$[\boldsymbol{g}_1(\boldsymbol{y})\ \boldsymbol{g}_2(\boldsymbol{y})\ \boldsymbol{g}_3(\boldsymbol{y})\ \boldsymbol{g}_4(\boldsymbol{y})\ \boldsymbol{g}_5(\boldsymbol{y})],$$

but it makes the last row vanish in both cases. This fact leads to the following equivalent formulation with a smaller number of state variables:

$$A = \begin{bmatrix} -k_1 & k_2 & 0 & 0 \\ k_1 & -k_2-k_3 & k_4 & 0 \\ -k_9 & k_3-k_9 & -k_4-k_5-k_9-k_{10} & k_6-k_9 \\ -k_8 & -k_8 & k_5-k_8 & -k_6-k_7-k_8 \end{bmatrix},$$

$$\boldsymbol{f}(\boldsymbol{y}) = \begin{bmatrix} 0\ 0\ k_9 L\ k_8 L \end{bmatrix}^\top, \qquad \boldsymbol{y} = \begin{bmatrix} y_1\ y_2\ y_3\ y_4 \end{bmatrix}^\top,$$

$$\begin{bmatrix} \boldsymbol{g}_1(\boldsymbol{y})\ \boldsymbol{g}_2(\boldsymbol{y})\ \boldsymbol{g}_3(\boldsymbol{y})\ \boldsymbol{g}_4(\boldsymbol{y})\ \boldsymbol{g}_5(\boldsymbol{y}) \end{bmatrix}$$

$$= \begin{bmatrix} -1&0&0&0&0 \\ 1&-1&0&0&0 \\ 0&1&-1&0&1 \\ 0&0&1&-1&0 \end{bmatrix} \operatorname{diag} \begin{pmatrix} \sqrt{k_1 y_1 + k_2 y_2} \\ \sqrt{k_3 y_2 + k_4 y_3} \\ \sqrt{k_5 y_3 + k_6 y_4} \\ \sqrt{k_7 y_4 + k_8 (L - \sum_{i=1}^{4} y_i)} \\ \sqrt{k_9 (L - \sum_{i=1}^{4} y_i) + k_{10} y_3} \end{pmatrix}$$

with $y_5(t) = L - \sum_{i=1}^{4} y_i(t)$.

As (3.4) is always satisfied in this formulation, the projection method will be used to keep the non-negativity of the components of the solution. Figure 3.1 indicates

how the projection method works at a certain time step for this formulation. The oblique solid or dotted line represents the hyperplane given by (3.4). The round point is the value at some time step of the unreflected process, which has a negative i-th component. The star point is the projection of this point onto D.

3.3 Numerical experiments

In order to see how well the SEE scheme behaves, we perform numerical experiments. As the dimension of the matrix A is not too large in our problems, we can diagonalize the matrix [21] for numerical calculations. Assume that we have a diagonal matrix Λ and a diagonalization matrix R such that

$$\Lambda = \mathrm{diag}(\lambda_1, \lambda_2, \lambda_3, \lambda_4), \qquad AR = R\Lambda.$$

Then, in (2.7), (2.8) or (2.11) we have

$$\begin{aligned} &\mathrm{e}^{Ah} = R\mathrm{diag}\left(\mathrm{e}^{\lambda_1 h}, \mathrm{e}^{\lambda_2 h}, \mathrm{e}^{\lambda_3 h}, \mathrm{e}^{\lambda_4 h}\right) R^{-1}, \\ &A^{-1}\left(\mathrm{e}^{Ah} - I\right) = R\mathrm{diag}\left(\frac{\mathrm{e}^{\lambda_1 h}-1}{\lambda_1}, \frac{\mathrm{e}^{\lambda_2 h}-1}{\lambda_2}, \frac{\mathrm{e}^{\lambda_3 h}-1}{\lambda_3}, \frac{\mathrm{e}^{\lambda_4 h}-1}{\lambda_4}\right) R^{-1}. \end{aligned}$$

Note that once we calculate these for a given h, we can use them for every step and trajectory.

In the sequel, we investigate the root mean square error (RMSE) in (2.12) by simulating 1000 independent trajectories for a given h. We also investigate computational costs. In the simulation results, we will indicate $S_a \stackrel{\text{def}}{=} n_e + n_r$, where n_e and n_r stand for the number of evaluations on the drift or diffusion coefficients and the number of generated pseudo random numbers, respectively. As we do not know the exact solution of the SDE in our problem, we will seek a numerical solution by the Milstein scheme [29] with $h = 2^{-10}$ and use it instead of the exact solution [37]. The Milstein scheme will be used only for this because it is very costly in our problem due to approximations to stochastic double integrals and the derivatives of the diffusion coefficients. For the approximations to stochastic double integrals, we can use the algorithm proposed by Wiktorsson [43] as in [31,37].

Our simulation strategy is as follows. We have 10 groups each of which has 100 trajectories. For them, we seek

$$\bar{\varepsilon}_j \stackrel{\text{def}}{=} \frac{1}{100}\sum_{l=1}^{100}\left\|\boldsymbol{y}_M(j,l) - \boldsymbol{y}_M^{\mathrm{Mil}}(j,l)\right\|^2 \qquad (j = 1,2,\ldots,10),$$

where $\boldsymbol{y}_M^{\mathrm{Mil}}(j,l)$ and $\boldsymbol{y}_M(j,l)$ stand for an approximation on the lth trajectory in the jth group, by the Milstein scheme and another scheme, respectively. Using them, we seek

$$\hat{\varepsilon} \stackrel{\text{def}}{=} \frac{1}{10}\sum_{j=1}^{10}\bar{\varepsilon}_j, \qquad \hat{\sigma}^2 \stackrel{\text{def}}{=} \frac{1}{9}\sum_{j=1}^{10}(\bar{\varepsilon}_j - \hat{\varepsilon})^2.$$

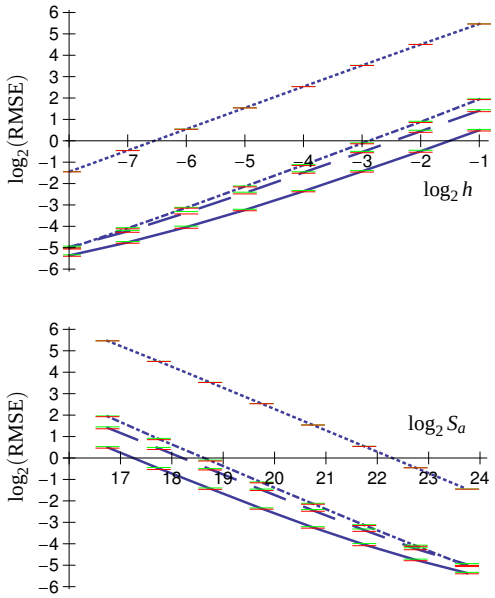

Fig. 3.2 Log-log plots of the RMSE of $\boldsymbol{y}(5)$ versus h or S_a (Solid: SEE, dash-dotted: EM, dotted: SLE, dash: SETD0)

Finally, we obtain a 90% confidence interval $(\hat{\varepsilon}-\triangle\hat{\varepsilon},\hat{\varepsilon}+\triangle\hat{\varepsilon})$ for $E[\|\boldsymbol{y}_M-\boldsymbol{y}(T)\|^2]$, where

$$\triangle\hat{\varepsilon} \stackrel{\text{def}}{=} 1.83\sqrt{\frac{\hat{\sigma}^2}{10}}$$

(see also [29, p. 46]). In figures, we will plot $(1/2)\log_2\hat{\varepsilon}$ with bars, which show $(1/2)\log_2(\hat{\varepsilon}-\triangle\hat{\varepsilon})$ and $(1/2)\log_2(\hat{\varepsilon}+\triangle\hat{\varepsilon})$.

The first is a case in which many reflections occur. We set parameters and an initial condition as follows:

$$k_1=0.2,\quad k_2=\frac{k_1}{50},\quad k_i=k_1\quad(i=3,4,\ldots,10),\quad L=400,$$
$$y_1(0)=y_3(0)=y_5(0)=100\quad(\text{w. p. }1),\quad y_2(0)=y_4(0)=50\quad(\text{w. p. }1).$$

The root mean square errors (RMSEs) are indicated in Figure 3.2. As the solution is a vector, the Euclidean norm is used. The solid, dash-dotted, dotted or dash lines denote the SEE scheme, the EM scheme, the SLE scheme or the SETD0 scheme, respectively. We can see that the SEE scheme is the best, whereas the SLE scheme is the worst. On the other hand, Figure 3.3 indicates the number of reflections per step over 1000 trajectories. We can see that there is not a large difference in the number of reflections.

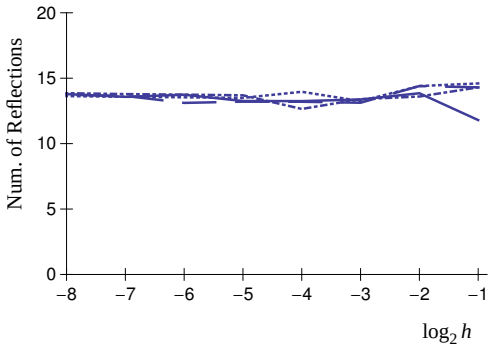

Fig. 3.3 Number of reflections per step over 1000 trajectories versus $\log_2 h$ (Solid: SEE, dash-dotted: EM, dotted: SLE, dash: SETD0)

The second problem is a stiff one depending on the value of k_1. We set the other parameters as follows:

$$k_2 = k_1, \quad k_i = 0.5 \quad (i = 3,4,\ldots,10).$$

The initial condition is the same as in the previous case. For several values of k_1, RMSEs are indicated in Figure 3.4. As k_1 becomes large, the SDE becomes increasingly stiff. When k_1=50, for example, we need a small step size h for the EM scheme to solve the SDE numerically stably. This is because one of the eigenvalues of A is -100.252. (Remember Figure 2.2.) On the other hand, for the SEE scheme we do not need such a small h as it is A-stable. The SLE and SETD0 schemes also do not require a small h for stability. Incidentally, Figure 3.5 indicates the RMSE versus the computational cost and the number of reflections when $k_1 = 50$. In Table 3.1, the schemes are compared in terms of CPU time to solve the same SDE. It has been measured by Intel C++ Compiler on Windows 7, Intel Core i7 CPU, 2.80 GHz. From these results, we can see that the SEE scheme has the best performance not only with respect to RMSEs versus h, but also in terms of computational costs and CPU time versus errors.

Table 3.1 CPU time to solve the SDE when $k_1 = 50$ (the unit is seconds)

$\log_2 h$	-1	-2	-3	-4	-5	-6	-7	-8
SSE	112	116	122	149	155	168	185	194
EM	—	—	—	—	—	166	186	195
SLE	112	117	123	154	157	170	185	199
SETD0	112	115	122	149	155	166	183	193

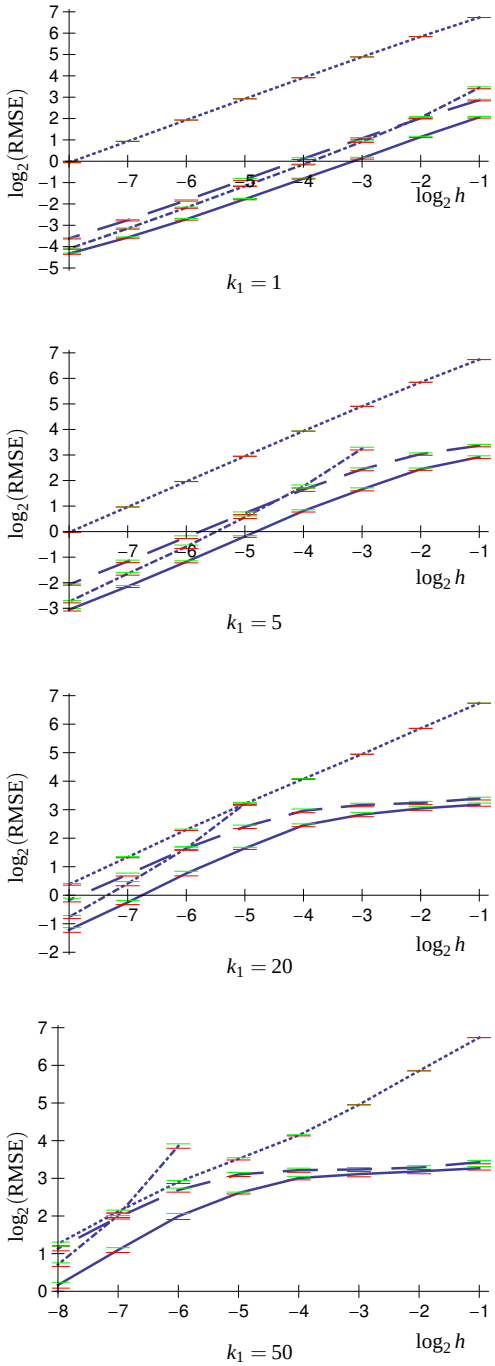

Fig. 3.4 Log-log plots of the RMSE of $\boldsymbol{y}(5)$ versus h for several values of k_1 (Solid: SEE, dash-dotted: EM, dotted: SLE, dash: SETD0)

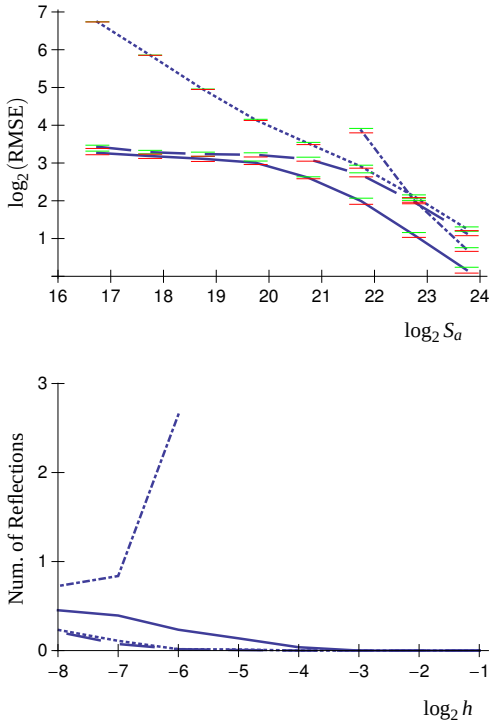

Fig. 3.5 Log-log plots of the RMSE of $\boldsymbol{y}(5)$ versus S_a, and the number of reflections per step over 1000 trajectories versus $\log_2 h$ when $k_1 = 50$ (Solid: SEE, dash-dotted: EM, dotted: SLE, dash: SETD0)

4 Conclusions

For non-commutative Itô SDEs with a semilinear drift term, we have derived the SEE scheme, which is of strong order one half. Using the scalar test SDE with complex coefficients, we have investigated stability properties for the scheme and have shown that it is A-stable in MS.

For numerical experiments we have dealt with the model for a K^+ channel that is computationally efficient [15], and have carried out the state space reduction for it. Then, using the reflection technique to keep the non-negativity of the numerical solutions, we have confirmed the advantages of the SEE scheme in the numerical experiments. Whereas the EM scheme has suffered from poor stability properties and the SLE scheme has always indicated low accuracy, the SEE scheme has shown the best performance in accuracy, computational costs and stability.

Acknowledgements The authors would like to thank the referees for their valuable and careful comments which helped them to improve the earlier versions of this paper.

References

1. Abdulle, A.: Fourth order Chebyshev methods with recurrence relation. SIAM J. Sci. Comput. **23**(**6**), 2041–2054 (2002)
2. Abdulle, A., Cirilli, S.: S-ROCK: Chebyshev methods for stiff stochastic differential equations. SIAM J. Sci. Comput. **30**(**2**), 997–1014 (2008)
3. Abdulle, A., Li, T.: S-ROCK methods for stiff Itô SDEs. Commun. Math. Sci. **6**(**4**), 845–868 (2008)
4. Abdulle, A., Medovikov, A.A.: Second order Chebyshev methods based on orthogonal polynomials. Numer. Math. **90**, 1–18 (2001)
5. Adamu, I.A.: Numerical approximation of SDEs and stochastic Swift-Hohenberg equation. Ph.D. thesis, Heriot-Watt University (2011)
6. Alfonsi, A.: High order discretization schemes for the CIR process: application to affine term structure and Heston models. Math. Comp. **79**(**269**), 209–237 (2010)
7. Arnold, L.: Stochastic Differential Equations: Theory and Applications. John Wiley & Sons, New York (1974)
8. Bayer, C., Szepessy, A., Tempone, R.: Adaptive weak approximation of reflected and stopped diffusions. Monte Carlo Methods Appl. **16**(**1**), 1–67 (2010)
9. Biscay, R., Jimenez, J.C., Riera, J.J., Valdes, P.A.: Local linearization method for numerical solution of stochastic differential equations. Ann. Inst. Statist. Math. **48**(**4**), 631–644 (1996)
10. Brennan, T., Fink, M., Rodriguez, B.: Multiscale modelling of drug-induced effects on cardiac electrophysiological activity. Eur. J. Pharm. Sci. **36**(**1**), 62–77 (2009)
11. Butcher, J.C.: Numerical Methods for Ordinary Differential Equations, second edn. John Wiley & Sons, Chichester (2008)
12. Carbonell, F., Jimenez, J.C., Biscay, R.J.: Weak local linear discretizations for stochastic differential equations: Convergence and numerical schemes. J. Comput. Appl. Math. **197**(**2**), 578–596 (2006)
13. Chen, Y., Ye, X.: Projection onto a simplex. e-print (2011). ArXiv:1101.6081v2
14. Cruz, d.l., Biscay, R.J., Jimenez, J.C., Carbonell, F., Ozaki, T.: High order local linearization methods: An approach for constructing A-stable explicit schemes for stochastic differential equations with additive noise. BIT **50**(**3**), 509–539 (2010)
15. Dangerfield, C., Kay, D., Burrage, K.: Modeling ion channel dynamics through reflected stochastic differential equations. Phys. Rev. E **85**, 051907, 15 pages (2012)
16. Ehle, B.L., Lawson, J.D.: Generalized Runge-Kutta processes for stiff initial-value problems. IMA J. Appl. Math. **16**(**1**), 11–21 (1975)
17. Gillespie, D.T.: The chemical Langevin equation. J. Chem. Phys. **113**(**1**), 297–306 (2000)
18. Higham, D.J.: A-stability and stochastic mean-square stability. BIT **40**(**2**), 404–409 (2000)
19. Hochbruck, M., Lubich, C., Selhofer, H.: Exponential integrators for large systems of differential equations. SIAM J. Sci. Comput. **19**(**5**), 1552–1574 (1998)
20. Hochbruck, M., Ostermann, A.: Explicit exponential Runge-Kutta methods for semilinear parabolic problems. SIAM J. Numer. Anal. **43**(**3**), 1069–1090 (2005)
21. Hochbruck, M., Ostermann, A.: Exponential integrators. Acta Numer. **19**, 209–286 (2010)
22. van der Houwen, P.J., Sommeijer, B.P.: On the internal stability of explicit *m*-stage Runge-Kutta methods for large *m*-values. Z. Angew. Math. Mech. **60**, 479–485 (1980)
23. Ilie, S., Morshed, M.: Automatic simulation of the chemical Langevin equation. Appl. Math. **4**(**1A**), 235–241 (2013)
24. Jentzen, A., Kloeden, E.: Overcoming the order barrier in the numerical approximation of stochastic partial differential equations with additive space-time noise. In: Proc. R. Soc. Lond. Ser. A Math. Phys. Eng. Sci. 465, pp. 649–667 (2009)
25. Jimenez, J.C.: A simple algebraic expression to evaluate the local linearization schemes for stochastic differential equations. Appl. Math. Lett. **15**(**6**), 775–780 (2002)
26. Jimenez, J.C., Cruz, d.l.: Convergence rate of strong local linearization schemes for stochastic differential equations with additive noise. BIT **52**(**2**), 357–382 (2012)
27. Jimenez, J.C., Shoji, I., Ozaki, T.: Simulation of stochastic differential equations through the local linearization method. a comparative study. J. Stat. Phys. **94**(**3-4**), 587–602 (1999)
28. Kiehn, J., Lacerda, A.E., Brown, A.M.: Pathways of herg inactivation. Am. J. Physiol. Heart Circ. Physiol. **277**(**1**), 199–210 (1999)
29. Kloeden, P.E., Platen, E.: Numerical Solution of Stochastic Differential Equations. Springer, New York (1999). Corrected Third Printing

30. Komori, Y., Burrage, K.: Weak second order S-ROCK methods for Stratonovich stochastic differential equations. J. Comput. Appl. Math. **236**(**11**), 2895–2908 (2012)
31. Komori, Y., Burrage, K.: Strong first order S-ROCK methods for stochastic differential equations. J. Comput. Appl. Math. **242**, 261–274 (2013)
32. Lawson, J.D.: Generalized Runge-Kutta processes for stable systems with large Lipschitz constants. SIAM J. Numer. Anal. **4**(**3**), 372–380 (1967)
33. Mélykúti, B., Burrage, K., Zygalakis, K.C.: Fast stochastic simulation of biochemical reaction systems by alternative formulations of the chemical Langevin equation. J. Chem. Phys. **132**(**16**), 164109 (2010)
34. Mora, C.M.: Weak exponential schemes for stochastic differential equations with additive noise. IMA J. Numer. Anal. **25**(**3**), 486–506 (2005)
35. Pettersson, R.: Approximations for stochastic differential equations with reflecting convex boundaries. Stochastic Process. Appl. **59**(**2**), 295–308 (1995)
36. Pope, D.: An exponential method of numerical integration of ordinary differential equations. Comm. ACM **6**(**8**), 491–493 (1963)
37. Rößler, A.: Runge-Kutta methods for the strong approximation of solutions of stochastic differential equations. SIAM J. Numer. Anal. **48**(**3**), 922–952 (2010)
38. Shi, C., Xiao, Y., Zhang, C.: The convergence and MS stability of exponential Euler method for semilinear stochastic differential equations. Abstr. Appl. Anal. **2012** (2012). 35040701, 19 pages
39. Shoji, I.: A note on convergence rate of a linearization method for the discretization of stochastic differential equations. Commun. Nonlinear Sci. Numer. Simul. **16**(7), 2667–2671 (2011)
40. Skorohod, A.V.: Stochastic equations for diffusion processes with a boundary. Theory Probab. Appl. **6**, 287–298 (1961)
41. Skorohod, A.V.: Stochastic equations for diffusion processes with boundaries. II. Theory Probab. Appl. **7**, 5–25 (1962)
42. Tanaka, H.: Stochastic differential equations with reflecting boundary condition in convex regions. Hiroshima Math. J. **9**(1), 163–177 (1979)
43. Wiktorsson, M.: Joint characteristic function and simultaneous simulation of iterated Itô integrals for multiple independent Brownian motions. The Annals of Prob. **11**(2), 470–487 (2001)